Eur. Phys. J. D **22**, 365–371 (2003)
DOI: 10.1140/epjd/e2003-00016-x

THE EUROPEAN PHYSICAL JOURNAL D

Interferometry with entangled atoms

U. Yurtsever, D. Strekalov, and J.P. Dowling[a]

Quantum Computing Technologies Group, Sec. 367, Jet Propulsion Laboratory, California Institute of Technology, 4800 Oak Grove Drive, Pasadena, California 91109-8099, USA

Received 6 June 2002 / Received in final form 25 October 2002
Published online 28 January 2003

Abstract. A quantum gravity-gradiometer consists of two spatially separated ensembles of atoms interrogated by pulses of a common laser beam. The laser pulses cause the probability amplitudes of atomic ground-state hyperfine levels to interfere, producing two, motion-sensitive, phase shifts, which allow the measurement of the average acceleration of each ensemble, and, via simple differencing, of the acceleration gradient. Here we propose entangling the quantum states of atoms from the two ensembles prior to the pulse sequence, and show that entanglement encodes their relative acceleration in a single interference phase which can be measured directly, with no need for differencing.

PACS. 39.20.+q Atom interferometry techniques – 03.75.Dg Atom and neutron interferometry – 03.67.-a Quantum information – 03.67.Lx Quantum computation

1 Introduction

Inertial sensors based on matter-wave interferometry are a rapidly developing technology [1–4]. One class of such sensors are gradiometers designed to measure linear acceleration gradients, typically gradients caused by inhomogeneities in the gravitational potential. The state-of-the-art design [4] for an atom-wave gravity gradiometer consists of a pair of atom-wave accelerometers separated spatially by a fixed distance and direction. Each of the two accelerometers contains an ensemble of laser-cooled atoms, through which a common pair of (counter-propagating) Raman laser beams are pulsed in a carefully controlled sequence to drive Rabi oscillations between atomic ground-state hyperfine levels. The sequence and timing of the laser pulses are adjusted so that the hyperfine ground and excited states of any single atom interfere during the atom's motion through the laser field. At the end of the sequence, the probability of finding an atom in its excited hyperfine state is a simple function of a relative phase, which accumulates between successive pulses in proportion to the atom's acceleration (relative to the inertial frame defined by the laser beam) averaged over its flight time. Subsequently, the resulting pair of observations of this phase (one for each ensemble) can be subtracted to obtain a measurement of the relative acceleration, and, upon dividing the result by the separation length, a measurement of the acceleration gradient. We will give a more quantitative review of this quantum interferometry technique in Section 2. A detailed description of the experimental setup can be found in [4] (see esp. Fig. 1 there).

Even though subtracting the two acceleration measurements allows a number of correlated noise sources to cancel out as common modes [4], it is still desirable to avoid such differencing of two nearly-equal measured quantities, which are corrupted by (uncorrelated) noise. In this paper, we will show that by prior-entangling (prior to the laser pulsing sequence) the quantum states of atoms in the two ensembles (such that every entangled pair has one atom in each ensemble) it becomes possible to encode the relative-acceleration information directly in a single interference phase, thereby eliminating the need for the differencing of two separate phase measurements. This idea is inspired by the recent discovery of a similar quantum algorithm which uses entangled states to synchronize atomic clocks non-locally [5]. The Quantum Clock Synchronization (QCS) algorithm relies on preparing the atoms "stabilizing" each atomic clock in a special entangled quantum state whose time evolution reduces to a pure multiplicative phase as long as each atom in the pair evolves under the same unitary transformation. By contrast, the Entangled Quantum Interferometry (EQI) algorithm to be described below relies on transforming the pair's quantum state into a sensor which senses the *difference* between unitary evolutions of the entangled atoms. Put another way, the EQI algorithm is a spatial analogue of the QCS algorithm, in exactly the same sense as atomic clocks are temporal analogues of quantum (atom-wave) interferometers [6].

[a] e-mail: jonathan.p.dowling@jpl.nasa.gov

2 Overview of matter-wave gravity gradiometry

Consider an atom in its internal ground state $|0\rangle$, moving through the inertial frame defined by the Raman beams of an atom interferometer. [Here "inertial frame" has the same meaning as in general relativity: in the presence of a gravitational field, our coordinate system will always be locally-Minkowski (free-falling, or geodesic-normal coordinates) so that the gravitational potential and its first derivatives vanish at the origin.] The wave function can be written as a tensor product of the atom's internal and external Hilbert-space states:

$$\begin{aligned}\Psi_{0:\mathbf{p}}(\mathbf{x},t) &= |0\rangle \otimes \int a(\mathbf{k},\omega)\, \mathrm{e}^{\mathrm{i}(\mathbf{k}\cdot\mathbf{x}-\omega t)}\, \mathrm{d}^3k \\ &\equiv |0\rangle \otimes \psi(\mathbf{x},t), \end{aligned} \tag{1}$$

where $a(\mathbf{k},\omega)$ defines the wave packet representing the external (space-time) part $\psi(\mathbf{x},t)$ of the quantum state, ω is related to $\mathbf{k}$ *via* the usual dispersion relation (plus an additive constant corresponding to the atom's internal energy level), and $\mathbf{p}$ denotes the average (in general time-dependent) momentum:

$$\mathbf{p} \equiv \langle\psi| -\mathrm{i}\hbar\nabla|\psi\rangle = (2\pi)^3 \int \hbar\mathbf{k}\, |a(\mathbf{k},\omega)|^2\, \mathrm{d}^3k. \tag{2}$$

The need for this cumbersome subscript notation $\Psi_{0:\mathbf{p}}$ will become clear in a moment. Since the two Raman beams are detuned in frequency by an amount Ω which corresponds to the energy difference between the ground and excited states $|0\rangle$ and $|1\rangle$, they might stimulate the ground-state atom to absorb a photon from one beam and emit a lower frequency photon into the other, resulting in a transition to the excited state $|1\rangle$. This stimulated transition gives the atom a net momentum kick in the amount $\hbar(\mathbf{k}_1 - \mathbf{k}_2) \equiv \hbar\mathbf{K}$, where $\mathbf{k}_1$, $\mathbf{k}_2$ ($|\mathbf{k}_1| > |\mathbf{k}_2|$) denote the wave vectors corresponding to the (counter-propagating) Raman beams. [As the vectors $\mathbf{k}_i$, $i = 1,\ 2$, point in opposite directions, the magnitude of $\mathbf{K}$ is typically twice that of the $\mathbf{k}_i$. Note that Ω is the *total* energy absorbed by the atom, which includes not only the transition energy (within the appropriate bandwidth), but also the recoil contribution.] The wave function of the same atom excited in this way from its ground state can then be decomposed, similarly to equation (1), in the form

$$\begin{aligned}\Psi_{1:\mathbf{p}+\hbar\mathbf{K}}(\mathbf{x},t) &= |1\rangle \otimes \int a(\mathbf{k},\omega)\, \mathrm{e}^{\mathrm{i}[(\mathbf{k}+\mathbf{K})\cdot\mathbf{x}-(\omega+\Omega)t]}\, \mathrm{d}^3k \\ &= |1\rangle \otimes \psi(\mathbf{x},t)\, \mathrm{e}^{\mathrm{i}(\mathbf{K}\cdot\mathbf{x}-\Omega t)}. \end{aligned} \tag{3}$$

Since the wave packet $\psi(\mathbf{x},t)$ is common to both the ground and excited state wave functions, we will suppress it (as an overall "normalization" factor) in what follows. Note that whenever an atom interrogated in the interferometer is excited from its ground state $|0:\mathbf{p}\rangle$ to the internal excited state $|1\rangle$ by Raman pulses, it always picks up an associated excess energy-momentum $(\mathbf{K},\Omega)$ as specified in equation (3); in other words, the excited atom's total quantum state becomes $|1:\mathbf{p}+\hbar\mathbf{K}\rangle$. Conversely, a stimulated transition in the reverse direction results in the transformation $|1:\mathbf{p}\rangle \longrightarrow |0:\mathbf{p}-\hbar\mathbf{K}\rangle$.

In the interferometer, atoms are manipulated by laser pulses of two basic kinds: A Hadamard pulse $H_{\frac{\pi}{2}}$ (a $\pi/2$ pulse followed by the spin operator σ_z), whose action is

$$\begin{aligned} H_{\frac{\pi}{2}}|0:\mathbf{p}\rangle &= \frac{1}{\sqrt{2}}(|0:\mathbf{p}\rangle + |1:\mathbf{p}+\hbar\mathbf{K}\rangle), \\ H_{\frac{\pi}{2}}|1:\mathbf{p}+\hbar\mathbf{K}\rangle &= \frac{1}{\sqrt{2}}(|0:\mathbf{p}\rangle - |1:\mathbf{p}+\hbar\mathbf{K}\rangle), \end{aligned} \tag{4}$$

and a "double" Hadamard pulse H_π (a π pulse followed by the spin operator σ_z), whose action is

$$\begin{aligned} H_\pi|0:\mathbf{p}\rangle &= |1:\mathbf{p}+\hbar\mathbf{K}\rangle, \\ H_\pi|1:\mathbf{p}+\hbar\mathbf{K}\rangle &= |0:\mathbf{p}\rangle\cdot \end{aligned} \tag{5}$$

Consider a single atom's flight across the laser field during the interrogation phase: initially, at times $t < t_1$, say, the atom is in the ground state $|0:\mathbf{p}\rangle$. At time $t = t_1$ the first $H_{\frac{\pi}{2}}$ pulse hits, and the atom's state becomes (up to an overall phase factor which we will always ignore):

$$\Psi(t_1) = \frac{1}{\sqrt{2}}\,(\,|0:\mathbf{p}\rangle + |1:\mathbf{p}+\hbar\mathbf{K}\rangle\,)\cdot \tag{6}$$

Since atoms are well-localized spatially, their wave functions $\Psi(\mathbf{x},t)$ are sharply peaked around their average position $\langle\Psi(t)|\,\mathbf{x}\,|\Psi(t)\rangle$ at all times t. When an atom is excited by Raman pulses to a superposition of its internal states, its distribution becomes bimodal, but still sharply peaked around the two positions (modes). Therefore, to a very good approximation, we can follow the evolution of the atom's wave function during its flight in the interferometer by examining it in the vicinity of the atom's (average) position(s) as a function of time t. (See [7] for a more rigorous treatment.) Accordingly, at any time t after t_1 and before the next Raman pulse hits, the state equation (6) evolves, according to equations (1–3), as

$$\Psi(t) = \frac{1}{\sqrt{2}}\left[|0:\mathbf{p}\rangle + \mathrm{e}^{\mathrm{i}\mathbf{K}\cdot(\mathbf{x}_t-\mathbf{x}_1)-\mathrm{i}\Omega(t-t_1)}|1:\mathbf{p}+\hbar\mathbf{K}\rangle\right], \qquad \forall t\colon t_1 \le t < t_2, \tag{7}$$

where $\mathbf{x}_t \equiv \mathbf{x}(t)$, $\mathbf{x}_1 \equiv \mathbf{x}(t_1)$ etc. is shorthand notation for the atom's position at the different times, and an overall phase factor as well as the common wave packet $\psi(\mathbf{x},t)$ are suppressed as advertised. At a time $t = t_2 > t_1$, an H_π pulse hits, and the atom's new state becomes

$$\Psi(t_2) = \frac{1}{\sqrt{2}}\left[|1:\mathbf{p}+\hbar\mathbf{K}\rangle + \mathrm{e}^{\mathrm{i}\mathbf{K}\cdot(\mathbf{x}_2-\mathbf{x}_1)-\mathrm{i}\Omega(t_2-t_1)}|0:\mathbf{p}\rangle\right]\cdot \tag{8}$$

At any time t after t_2 and before the next pulse, the state equation (8) evolves as

$$\Psi(t) = \frac{1}{\sqrt{2}}\left[\,\mathrm{e}^{\mathrm{i}\mathbf{K}\cdot(\mathbf{x}_t-\mathbf{x}_2)-\mathrm{i}\Omega(t-t_2)}|1:\mathbf{p}+\hbar\mathbf{K}\rangle + \mathrm{e}^{\mathrm{i}\mathbf{K}\cdot(\mathbf{x}_2-\mathbf{x}_1)-\mathrm{i}\Omega(t_2-t_1)}|0:\mathbf{p}\rangle\right], \qquad \forall t\colon t_2 \le t < t_3. \tag{9}$$

At time $t = t_3$, the second and last $H_{\frac{\pi}{2}}$ pulse hits, and transforms $\Psi(t)$ into the state

$$\Psi(t_3) = \frac{1}{2}\Big[\mathrm{e}^{\mathrm{i}\mathbf{K}\cdot(\mathbf{x}_3-\mathbf{x}_2)-\mathrm{i}\Omega(t_3-t_2)}(|0:\mathbf{p}\rangle - |1:\mathbf{p}+\hbar\mathbf{K}\rangle) + \mathrm{e}^{\mathrm{i}\mathbf{K}\cdot(\mathbf{x}_2-\mathbf{x}_1)-\mathrm{i}\Omega(t_2-t_1)}(|0:\mathbf{p}\rangle + |1:\mathbf{p}+\hbar\mathbf{K}\rangle)\Big]\cdot \quad (10)$$

So as a result of the pulse sequence $H_{\frac{\pi}{2}} - H_\pi - H_{\frac{\pi}{2}}$, an atom which enters the interferometer in the ground state $|0:\mathbf{p}\rangle$ ends up, at the end of the last $H_{\frac{\pi}{2}}$ pulse (at $t = t_3$), in the state equation (10) which can be rewritten as

$$\Psi(t_3) = \frac{1}{2}\left[\left(\mathrm{e}^{\mathrm{i}\Theta_{21}} + \mathrm{e}^{\mathrm{i}\Theta_{32}}\right)|0:\mathbf{p}\rangle + \left(\mathrm{e}^{\mathrm{i}\Theta_{21}} - \mathrm{e}^{\mathrm{i}\Theta_{32}}\right)|1:\mathbf{p}+\hbar\mathbf{K}\rangle)\right], \quad (11)$$

where for $i, j = 1, 2, 3, \ldots$

$$\Theta_{ij} \equiv \mathbf{K}\cdot(\mathbf{x}_i - \mathbf{x}_j) - \Omega(t_i - t_j). \quad (12)$$

After absorbing a factor of $\mathrm{e}^{\mathrm{i}\Theta_{21}}$ into the overall phase multiplying $\Psi(t_3)$, equation (11) takes the more familiar form

$$\Psi(t_3) = \frac{1}{2}\left[\left(1+\mathrm{e}^{\mathrm{i}\Theta}\right)|0:\mathbf{p}\rangle + \left(1-\mathrm{e}^{\mathrm{i}\Theta}\right)|1:\mathbf{p}+\hbar\mathbf{K}\rangle)\right], \quad (13)$$

where $\Theta \equiv \Theta_{32} - \Theta_{21}$. The phase Θ can now be observed by measuring the relative abundance of ground *vs.* excited state atoms in the state $\Psi(t_3)$. Specifically, the fraction P_1 of excited-state atoms in the state equation (13) is given by

$$P_1 = \frac{1}{4}\left|1-\mathrm{e}^{\mathrm{i}\Theta}\right|^2 = \sin^2\left(\frac{\Theta}{2}\right), \quad (14)$$

and, similarly, the fraction P_0 of ground state atoms is $P_0 = |1+\mathrm{e}^{\mathrm{i}\Theta}|^2/4 = \cos^2(\Theta/2)$. On the other hand, substituting equations (12) in $\Theta = \Theta_{32} - \Theta_{21}$ gives

$$\Theta = \mathbf{K}\cdot[\mathbf{x}(t_3) - 2\mathbf{x}(t_2) + \mathbf{x}(t_1)] - \Omega(t_3 - 2t_2 + t_1). \quad (15)$$

If the Raman pulses making up the sequence $H_{\frac{\pi}{2}} - H_\pi - H_{\frac{\pi}{2}}$ are aligned in time such that $t_2 = t_1 + T$ and $t_3 = t_2 + T$ for some common interrogation time T, the second term in parenthesis in equation (15) vanishes, and, using the standard Taylor expansion of $\mathbf{x}(t)$, we can rewrite the first term in the form

$$\Theta = \mathbf{K}\cdot\ddot{\mathbf{x}}(t_2)\,T^2 \;+\; O\left(T^3\right). \quad (16)$$

Here the magnitude of the $O(T^3)$ remainder is down by a factor of order T/T_a relative to the first (acceleration) term, where $T_a \sim \|\mathbf{a}\|/\|\dot{\mathbf{a}}\|$ denotes the timescale over which the atom's acceleration $\mathbf{a}(t) \equiv \ddot{\mathbf{x}}(t)$ varies. Therefore, as long as the time scale T_a is much larger (as is typically the case) than the interrogation time T, measurement of the phase Θ following the pulse sequence $H_{\frac{\pi}{2}} \overline{\;T\;} H_\pi \overline{\;T\;} H_{\frac{\pi}{2}}$ yields a direct measurement [8] of the inertial acceleration component $\mathbf{K}\cdot\mathbf{a}$.

3 Interferometry with entangled atoms

For a gradient measurement, ordinarily it is necessary to apply two separate but simultaneous measurements of acceleration to two different ensembles of atoms separated spatially by a fixed distance. The differential acceleration obtained from these measurements is usually is much smaller than each locally found acceleration. Therefore the noise associated with each measurement can severely limit the accuracy of the gradient measurement. The necessity for subtracting two large numbers can be avoided, as will be shown in this section, by using atoms whose internal states are pairwise entangled in a distributed fashion. In this case it is possible to obtain the acceleration gradient information with just one phase measurement.

Start, at time $t = t_1$, with atoms A and B in the pairwise entangled initial state

$$\Psi(t_1) = \frac{1}{\sqrt{2}}\left(|0:\mathbf{p}_A\rangle_A\,|1:\mathbf{p}_B+\hbar\mathbf{K}\rangle_B - |1:\mathbf{p}_A+\hbar\mathbf{K}\rangle_A\,|0:\mathbf{p}_B\rangle_B\right)\cdot \quad (17)$$

Methods for producing this state will be discussed in the following sections. Since the state equation (17) is an energy eigenstate of the total internal Hamiltonian, its explicit time evolution consists of a pure multiplicative phase only. Implicitly, it evolves in time kinematically with the inertial motion of the atoms; according to equations (1–3), this evolution takes the form

$$\Psi(t) = \frac{1}{\sqrt{2}}\Big[\mathrm{e}^{\mathrm{i}\mathbf{K}\cdot(\mathbf{x}_{Bt}-\mathbf{x}_{B1})}\,|0:\mathbf{p}_A\rangle_A\,|1:\mathbf{p}_B+\hbar\mathbf{K}\rangle_B - \mathrm{e}^{\mathrm{i}\mathbf{K}\cdot(\mathbf{x}_{At}-\mathbf{x}_{A1})}\,|1:\mathbf{p}_A+\hbar\mathbf{K}\rangle_A\,|0:\mathbf{p}_B\rangle_B\Big], \quad \forall t\colon t_1 \le t < t_2, \quad (18)$$

where $\mathbf{x}_{At} \equiv \mathbf{x}_A(t)$, $\mathbf{x}_{B1} \equiv \mathbf{x}_B(t_1)$, etc., and an overall phase factor as well as the common wave packet $\psi_A(\mathbf{x}_A, t)\psi_B(\mathbf{x}_B, t)$ are suppressed as in equation (7) above. For increased readability, let us introduce the following abbreviation which we will use throughout the rest of this paper: for $E = A, B$,

$$|0\rangle_E \equiv |0:\mathbf{p}_E\rangle_E, \qquad |1\rangle_E \equiv |1:\mathbf{p}_E+\hbar\mathbf{K}\rangle_E. \quad (19)$$

Now suppose that, at a time $t = t_2 > t_1$, a *common* H_π pulse is applied to both atoms A and B (simultaneously) in the state equation (18). Then the new state of the pair at $t = t_2$ becomes

$$\Psi(t_2) = \frac{1}{\sqrt{2}}\Big[\mathrm{e}^{\mathrm{i}\mathbf{K}\cdot(\mathbf{x}_{B2}-\mathbf{x}_{B1})}\,|1\rangle_A\,|0\rangle_B - \mathrm{e}^{\mathrm{i}\mathbf{K}\cdot(\mathbf{x}_{A2}-\mathbf{x}_{A1})}\,|0\rangle_A\,|1\rangle_B\Big]\cdot \quad (20)$$

At any time t after t_2 and before the next pulse, the state equation (20) evolves as

$$\Psi(t) = \frac{1}{\sqrt{2}}\Big[\mathrm{e}^{\mathrm{i}\mathbf{K}\cdot(\mathbf{x}_{At}-\mathbf{x}_{A2}+\mathbf{x}_{B2}-\mathbf{x}_{B1})}\,|1\rangle_A\,|0\rangle_B - \mathrm{e}^{\mathrm{i}\mathbf{K}\cdot(\mathbf{x}_{Bt}-\mathbf{x}_{B2}+\mathbf{x}_{A2}-\mathbf{x}_{A1})}\,|0\rangle_A\,|1\rangle_B\Big], \quad \forall t\colon t_2 \le t < t_3. \quad (21)$$

At a time $t = t_3 > t_2$, a final, *common* $H_{\frac{\pi}{2}}$ pulse is applied to the entangled pair A and B, and transforms the state equation (21) into

$$\Psi(t_3) = \frac{1}{2\sqrt{2}} \Big[\mathrm{e}^{\mathrm{i}(\Phi^A_{32}+\Phi^B_{21})}(|0\rangle_A - |1\rangle_A)(|0\rangle_B + |1\rangle_B) - \mathrm{e}^{\mathrm{i}(\Phi^B_{32}+\Phi^A_{21})}(|0\rangle_A + |1\rangle_A)(|0\rangle_B - |1\rangle_B) \Big], \quad (22)$$

where, for $i, j = 1, 2, 3, \ldots$,

$$\Phi^A_{ij} \equiv \mathbf{K} \cdot (\mathbf{x}_{Ai} - \mathbf{x}_{Aj}), \;\; \Phi^B_{ij} \equiv \mathbf{K} \cdot (\mathbf{x}_{Bi} - \mathbf{x}_{Bj}). \quad (23)$$

After absorbing a factor of $\mathrm{e}^{\mathrm{i}(\Phi^B_{32}+\Phi^A_{21})}$ into the overall phase multiplying $\Psi(t_3)$, equation (22) takes the more manageable form

$$\Psi(t_3) = \frac{1}{2\sqrt{2}} \big[\mathrm{e}^{\mathrm{i}\Phi}(|0\rangle_A - |1\rangle_A)(|0\rangle_B + |1\rangle_B) - (|0\rangle_A + |1\rangle_A)(|0\rangle_B - |1\rangle_B) \big], \quad (24)$$

with the phase observable Φ given by

$$\Phi \equiv \Phi^A_{32} + \Phi^B_{21} - \Phi^B_{32} - \Phi^A_{21} = \mathbf{K} \cdot (\Delta\mathbf{x}_3 - 2\,\Delta\mathbf{x}_2 + \Delta\mathbf{x}_1), \quad (25)$$

where $\Delta\mathbf{x} \equiv \mathbf{x}_A - \mathbf{x}_B$ and $\Delta\mathbf{x}_i \equiv \mathbf{x}_{Ai} - \mathbf{x}_{Bi}$ for $i, j = 1, 2, 3, \ldots$ Collecting terms in equation (24),

$$\Psi(t_3) = \frac{1}{2\sqrt{2}} \big[(\mathrm{e}^{\mathrm{i}\Phi} - 1)|0\rangle_A|0\rangle_B + (\mathrm{e}^{\mathrm{i}\Phi} + 1)|0\rangle_A|1\rangle_B - (\mathrm{e}^{\mathrm{i}\Phi} + 1)|1\rangle_A|0\rangle_B - (\mathrm{e}^{\mathrm{i}\Phi} - 1)|1\rangle_A|1\rangle_B \big] \cdot \quad (26)$$

The phase Φ can now be observed by measuring the relative abundance in the state $\Psi(t_3)$ of those pairs in which both atoms are in their excited states. If the measurement is performed with a flux of atoms sufficiently low to entangle and probe one pair at a time, determining the instances when both atoms are excited can be easily done by selective ionization.

Even though $\Psi(t_3)$ is not stationary, its time evolution consists of pure phases multiplying each of the coefficients in equation (26), so the observation time is not critical. Specifically, according to equation (26), the fraction P_{11} of those pairs in which both the A-atom and the B-atom are in the excited state $|1\rangle$ is given by

$$P_{11} = \frac{1}{8}\left|\mathrm{e}^{\mathrm{i}\Phi} - 1\right|^2 = \frac{1}{2}\sin^2\left(\frac{\Phi}{2}\right) \cdot \quad (27)$$

On the other hand, if the Raman pulses making up the sequence $-H_\pi - H_{\frac{\pi}{2}}$ are aligned in time as before so that $t_2 = t_1 + T$ and $t_3 = t_2 + T$ for some common interrogation time T, we can write, using equation (25),

$$\Phi = \mathbf{K} \cdot \Delta\ddot{\mathbf{x}}(t_2)\, T^2 \; + \; O\left(T^3\right), \quad (28)$$

where the magnitude of the $O(T^3)$ remainder is again down by a factor of order T/T_a relative to the first (acceleration) term, with T_a denoting the timescale over which the atoms' acceleration varies. As long as the time scale T_a is much larger than the interrogation time T, measurement of the single phase observable Φ following the pulse sequence $\frac{}{T} H_\pi \frac{}{T} H_{\frac{\pi}{2}}$ on the entangled pair equation (17) yields a direct measurement of the inertial acceleration gradient $\mathbf{K} \cdot \Delta\mathbf{a} = \mathbf{K} \cdot (\mathbf{a}_A - \mathbf{a}_B)$ between the atoms A and B. Signal sensitivity of Φ to the acceleration gradient $\Delta\mathbf{a}$ can be enhanced using techniques similar to the one discussed in the note [8].

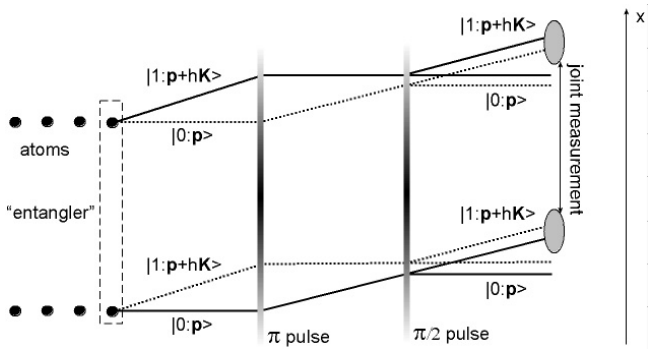

Fig. 1. Diagrammatics of our proposed concept for matter-wave interferometry with an ensemble of pairwise-entangled atoms.

Our concept of matter-wave interferometric gradiometry with entangled atoms is illustrated in Figure 1, where the dashed and solid lines represent two alternative trajectories of the entangled system. From this diagram we see the main distinction between our scheme and a variety of other proposals for atomic and optical interferometers, including those using entanglement: our scheme relies on pair-by-pair entanglement followed by pairwise detection, *i.e.* on a large ensemble of distinguishable pairs of entangled atoms, rather than on entanglement *between* large numbers of atoms (*e.g.* states of the form $|N\rangle|0\rangle + |0\rangle|N\rangle$) on which most other proposed schemes for entangled interferometry are founded. [See, for example [9] for (unentangled) atom-wave interferometers [10] for optical interferometers with entangled light, and [11] for producing entangled ensembles of atoms (although not specifically for interferometry).]

4 Quantifying the improvement

To what extent does the entangled-interferometry technique proposed in Section 3 represent an improvement over the standard, "classical" atom-wave gradiometry as reviewed in Section 2? To answer this question quantitatively, we will now carry out a simple analysis of the improvement in the signal-to-noise ratio expected with entangled-interferometry.

We will take the differential phase-shift as our observed signal, so in a gradient measurement with both classical and entangled interferometry, the signal is the dimensionless quantity

$$S = \mathbf{K} \cdot \Delta\mathbf{a}\, T^2, \quad (29)$$

where $\mathbf{a} \equiv \ddot{\mathbf{x}}$, and other symbols are defined as in equations (16, 28), with the same approximation that allows neglecting terms of order $O(T^3)$ being assumed implicitly. In this discussion, for ease of notation we will label the two atomic ensembles by $i = 1, 2$. In a "classical" gradient measurement, two ensembles containing M atoms each are used to obtain the two acceleration measurements, which are later differenced to obtain the signal

$$S = \Theta_1 - \Theta_2, \tag{30}$$

where the phase observables Θ_i are related to the observed abundance (fluorescence) of excited-state atoms in each ensemble $i = 1,\ 2$ *via* equation (14):

$$\sin^2\left(\frac{\Theta_i}{2}\right) = \frac{M_i}{M}\,. \tag{31}$$

Here M_i denotes the number of excited-state atoms at the end of the interrogation process in ensemble i, $i = 1, 2$.

For comparison, imagine a similar experiment using the entangled algorithm of Section 3, involving M pairs of entangled atoms interrogated in the pulse sequence of equations (17–23) with the same interrogation-time constant T. At the end of that sequence, the number of atom pairs M_{11} in which both atoms end up in their excited states is measured, which yields the signal

$$S = \Phi, \tag{32}$$

where according to equation (27)

$$\frac{1}{2}\sin^2\left(\frac{\Phi}{2}\right) = \frac{M_{11}}{M}\,. \tag{33}$$

For simplicity, we will now make the additional assumption that the only sources of noise in both kinds of signal measurements (classical and entangled) are (i) phase noise, and (ii) shot noise due to the statistical fluctuations in the observed numbers of excited atoms: in M_1 and M_2 for the classical case, and in M_{11} for the entangled case. Since in the latter case we entangle and probe the atoms pair-by-pair, it is reasonable to assume that the number of successfully prepared pairs M is known exactly. The same assumption will be made in the classical case for consistency of the comparison. We will assume a binomial distribution for these random variables with M trials and with probabilities P_1, P_2, and P_{11}, respectively. These probabilities include the detection efficiency of the ion counters as well as the effects of loss of atoms due to collisions, etc. The expected RMS shot noise in each number measurement M_i is then given by

$$\Delta M_i \equiv \sqrt{\langle {M_i}^2\rangle - \langle M_i\rangle^2} = \sqrt{P_i(1-P_i)M}, \tag{34}$$

and the expected RMS noise in M_{11} is, similarly,

$$\Delta M_{11} \equiv \sqrt{\langle {M_{11}}^2\rangle - \langle M_{11}\rangle^2} = \sqrt{P_{11}(1-P_{11})M}. \tag{35}$$

In the classical measurement (Eqs. (30, 31)), the shot noise contribution to each Θ_i measurement can be written as

$$N_i = \frac{\partial\Theta_i}{\partial M_i}\Delta M_i \quad i = 1,\ 2. \tag{36}$$

Since the two measurements of Θ_i are completely independent, the total variance (noise squared) in the quantity $S = \Delta\Theta$ is the sum of the variances in each Θ_i:

$$N_c = \left({N_1}^2 + {N_2}^2\right)^{\frac{1}{2}} \approx \sqrt{2}N_1 = \sqrt{2}\,\frac{\partial\Theta_1}{\partial M_1}\Delta M_1\ , \tag{37}$$

where the approximate equality holds because of the assumption that the signal $S \ll 1$. Substituting equations (31, 34, 14) in equation (37) gives

$$N_c = \left(\frac{2}{M}\right)^{\frac{1}{2}}. \tag{38}$$

In the entangled measurement, according to equations (32, 33)

$$S = \Phi = 2\arcsin\sqrt{\frac{2M_{11}}{M}} \approx 2\sqrt{2}\sqrt{\frac{M_{11}}{M}}, \tag{39}$$

and the shot noise contribution is

$$N_e = \frac{\partial\Phi}{\partial M_{11}}\Delta M_{11} = \left(\frac{2(1-p_{11})}{M}\right)^{\frac{1}{2}} \approx \left(\frac{2}{M}\right)^{\frac{1}{2}}, \tag{40}$$

where the second equality follows from equation (35), and the third by the assumption that the signal $S \ll 1$. Remarkably, the shot noise contributions in the classical and entangled measurements are identical. Since a typical classical gradient measurement operates in a regime where the number of atoms M in each ensemble i is large enough to make shot noise negligible [4], the same operating conditions will make it negligible also in the entangled case, and therefore phase noise is the dominant source of error in both kinds of measurement.

To compare phase-noise performance of the two kinds of measurement, we will model the noise as simply proportional to the magnitude of the fluorescence signal [4]:

$$\langle {\Theta_i}^2\rangle - \langle\Theta_i\rangle^2 = \sigma^2\sin^2\frac{\langle\Theta_i\rangle}{2}, \quad i = 1,\ 2 \tag{41}$$

for the classical case, and

$$\langle\Phi^2\rangle - \langle\Phi\rangle^2 = \sigma^2\frac{1}{2}\sin^2\frac{\langle\Phi\rangle}{2}, \quad i = 1,\ 2 \tag{42}$$

in the entangled case, where σ is a constant. By the same arguments as above (Eqs. (36, 37)), the phase noise in the differential acceleration signal is, for the classical case

$$N_c \approx \sqrt{2}\,\sigma\sin\frac{\langle\Theta_1\rangle}{2}, \tag{43}$$

and for the entangled case

$$N_e = \frac{1}{\sqrt{2}}\,\sigma\sin\frac{\langle\Phi\rangle}{2}\,. \tag{44}$$

Therefore the ratio of phase noise in the entangled measurement to that in the classical measurement can be written in the form (*cf.* Eqs. (32, 30, 29))

$$\frac{N_e}{N_c} = \frac{1}{2}\frac{\sin\frac{\langle\Phi\rangle}{2}}{\sin\frac{\langle\Theta_1\rangle}{2}} \approx \frac{1}{2}\frac{\langle\Phi\rangle}{\langle\Theta_1\rangle} \sim \frac{1}{2}\frac{\|\Delta\mathbf{a}\|}{\|\mathbf{a}\|}\,. \tag{45}$$

For a typical measurement performed on earth with a 1 m separation between the two atomic ensembles, the earth's $\sim 3\,000$ E gradient field (1 E $= 10^{-9}$ s^{-2}) and 1 g gravity suggests suppression of phase noise *via* entanglement by a factor of up to 1.5×10^{-7}, or more than six orders of magnitude. For measurements performed in spacecraft in low earth orbit, the ambient acceleration $\|\mathbf{a}\|$ will be due to non-isolated common-mode vibrations originating from drag forces acting on the spacecraft. Therefore, for a gradiometer in low earth orbit (common-mode accelerations due to atmospheric drag being typically of order 10^{-5} g or higher) the phase-noise suppression N_e/N_c *via* entangled interferometry can be expected to be a reduced but still significant two orders of magnitude or better.

5 Producing the entangled atom pairs

A number of methods for entangling two-level atoms have been discussed in the literature and some implemented in experiments. For completeness, we will sketch two such methods which can be used to produce states of the form equation (17).

One method, originally proposed in Cabrillo *et al.* [12], involves pumping two spatially separated atoms A and B into their excited states, so that the joint system is initially in the product state

$$|1\rangle_A|1\rangle_B.$$

A single-photon detector, which cannot (even in principle) distinguish the atom from which a detected photon arrives, is placed halfway between the atoms. Such a detection scheme can be implemented either by using a detector which is inherently insensitive to the direction of the photon that triggers it, or by using two detectors situated at the output ports of a symmetric beam-splitter on which the light paths from the two atoms are symmetrically impingent, thus erasing the which-path information. When one of the atoms makes a transition to its ground state, and the detector registers the emitted photon, the result of its measurement is to put the combined two-atom system into the entangled state

$$\frac{1}{\sqrt{2}}\left(|0\rangle_A|1\rangle_B + \mathrm{e}^{\mathrm{i}\phi}|1\rangle_A|0\rangle_B\right), \tag{46}$$

where the phase ϕ is a measure of the relative delay between the paths reaching the detectors from A *versus* from B, and can be adjusted to have any desired value (*e.g.* as in Eq. (17)) by adjusting the position of the detector relative to the atoms. The disadvantage of this method is that it requires perfect detectors capable of distinguishing a single photon from a photon pair. In practice, photon detectors normally do not have the photon-number resolution, and always have quantum efficiency significantly lower than unity. As a result, the state (46) will no longer be the maximally entangled pure state, but a mixed state that includes a fraction representing both atoms in the ground state, with the weight proportional to the probability of the detectors' failure to detect the second photon. This will lead to errors in the phase measurements.

A second method, recently investigated in detail by Haroche and coworkers [13] is (in very rough outline) the following: start with a single-mode cavity whose excitation frequency is tuned to Ω. Send the pair of atoms A and B into the cavity one after the other, with atom B first. Initially, both atoms and the cavity are in their ground states:

$$|0\rangle_A\,|0\rangle_B\,|0\rangle_{EM}, \tag{47}$$

where $|0\rangle_{EM}$ denotes the vacuum state of the cavity. After atom B is in the cavity, apply a $\pi/2$-pulse on it, which transforms the state equation (47) into

$$\frac{1}{\sqrt{2}}|0\rangle_A\,(|0\rangle_B\,|1\rangle_{EM} - |1\rangle_B|0\rangle_{EM})\,. \tag{48}$$

When both atoms are in the cavity, apply a second, π-pulse, this time on the atom A, thereby transforming the state equation (48) into

$$\frac{1}{\sqrt{2}}\,(\,|1\rangle_A\,|0\rangle_B\,-\,|0\rangle_A\,|1\rangle_B\,)\otimes|0\rangle_{EM}, \tag{49}$$

which, for the atom-pair A and B, is in the desired form equation (17) up to an overall phase factor. The problem with this method is that it is local. To apply it in our protocol, we would have to solve an additional problem of transporting the entangled atoms to the locations of the measurement without decoherence. However, considering that a number of proof-of-principle experiments confirming it have already been performed successfully [13], this method (or, more precisely, a suitable variant which maintains the necessary correlation between atomic energy levels and linear momentum as discussed Sect. 2 above) is likely to be the method of choice in practical implementations of the entangled-atom gradiometry algorithm.

6 Future work

The Entangled Quantum Interferometry algorithm as presented here can be generalized to design sensors of other "distributed" quantities (such as higher derivatives of the gravitational curvature tensor); these generalizations will be discussed in a future publication.

We would like to acknowledge valuable discussions with Lute Maleki and Nan Yu of the JPL Frequency Standards Laboratory, and with John Clauser and Colin Williams of the JPL Quantum Computing Technologies group. The research described in this paper was carried out at the Jet Propulsion Laboratory, California Institute of Technology, under

a contract with the National Aeronautics and Space Administration, and was supported by a contract with the National Reconnaissance Office.

References

1. *Atom Interferometry*, edited by P.R. Berman (Academic Press, New York, 1997)
2. M. Kasevich, S. Chu, Phys. Rev. Lett. **67**, 181 (1991)
3. M. Kasevich, S. Chu, Appl. Phys. B **54**, 321 (1992)
4. M.J. Snadden *et al.,* Phys. Rev. Lett. **81**, 971 (1998)
5. R. Jozsa, D.S. Abrams, J.P. Dowling, C.P. Williams, Phys. Rev. Lett. **85**, 2010 (2000)
6. D.J. Wineland, J.J. Bollinger, W.M. Itano, F.L. Moore, D.J. Heinzen, Phys. Rev. A **46**, R6797 (1992)
7. R. Friedberg, S.R. Hartmann, Phys. Rev. A **48**, 1446 (1993); P. Storey, C. Cohen-Tannoudji, J. Phys. II France **4**, 1999 (1994)
8. Signal sensitivity in this acceleration measurement can be improved by employing more complicated pulsing sequences. For example, consider the pulse sequence

   $$H_{\frac{\pi}{2}}\,\overline{0}\,H_{(\pi)}\,\overline{T}\,H_{(\pi)}\,\overline{0}\,H_{\pi}\,\overline{0}\,H_{(\pi)}\,\overline{T}\,H_{(\pi)}\,\overline{0}\,H_{\frac{\pi}{2}},$$

   where, for example, $H_{\frac{\pi}{2}}\,\overline{0}\,H_{(\pi)}$ denotes that the two successive pulses are supposed to be applied one after the other with zero time delay, and $H_{(\pi)}$ denotes the "minus-π" pulse defined by (*cf.* Eqs. (5))

   $$H_{(\pi)}|0:\mathbf{p}\rangle = |1:\mathbf{p}-\hbar\mathbf{K}\rangle,\ H_{(\pi)}|1:\mathbf{p}\rangle = |0:\mathbf{p}+\hbar\mathbf{K}\rangle.$$

   (An H_{π} pulse turns into to an $H_{(\pi)}$ pulse upon switching the detuning order of the two Raman beams in such a way that the sign flip $\mathbf{K} \longrightarrow -\mathbf{K}$ results.) Following through a calculation similar to the one between equations (6, 13), it is straightforward to show that an atom initially in the ground state $|0:\mathbf{p}\rangle$ ends up, at the end of the longer pulse sequence above, in a superposition state of the form equation (13) where the phase Θ is now given by $\Theta = 3\,\mathbf{K}\cdot\mathbf{a}\,T^2 + O(T^3)$. Hence a factor of 3 improvement in the acceleration signal compared to the sequence $H_{\frac{\pi}{2}}\,\overline{T}\,H_{\pi}\,\overline{T}\,H_{\frac{\pi}{2}}$ [see, for example [1] (p. 388) and references cited therein for a discussion on this and similar techniques for boosting detection sensitivity]
9. S.B. Cahn, A. Kumarakrishnan, U. Shim, T. Sleator, P.R. Berman, B. Dubetsky, Phys. Rev. Lett. **79**, 784 (1997)
10. G.M. D'Ariano, M.G.A. Paris, P. Perinotti, Phys. Rev. A **65**, 062106 (2002); A. Kuzmich, L. Mandel, Quant. Semiclass. Opt. **10**, 493 (1998)
11. L.M. Duan, M.D. Lukin, J.I. Cirac, P. Zoller, Nature **414**, 413 (2001)
12. C. Cabrillo, J.I. Cirac, P. Garcia-Fernandez, P. Zoller, Phys. Rev. A **59**, 1025 (1999)
13. E. Hagley, X. Maître, G. Nogues, C. Wunderlich, M. Brune, J.M. Raimond, S. Haroche, Phys. Rev. Lett. **79**, 1 (1997); A. Jabs, `http://xxx.lanl.gov/abs/quant-ph/9811042`; A. Rauschenbeutel, P. Bertet, S. Osnaghi, G. Nogues, M. Brune, J.M. Raimond, S. Haroche, `http://xxx.lanl.gov/abs/quant-ph/0105062`